

Complementarity reveals bound entanglement of two twisted photons

This content has been downloaded from IOPscience. Please scroll down to see the full text.

2013 New J. Phys. 15 083036

(<http://iopscience.iop.org/1367-2630/15/8/083036>)

View [the table of contents for this issue](#), or go to the [journal homepage](#) for more

Download details:

IP Address: 132.229.211.17

This content was downloaded on 09/05/2017 at 12:27

Please note that [terms and conditions apply](#).

You may also be interested in:

[Mutually unbiased bases and bound entanglement](#)

Beatrix C Hiesmayr and Wolfgang Löffler

[A geometric comparison of entanglement and quantum nonlocality in discrete systems](#)

Christoph Spengler, Marcus Huber and Beatrix C Hiesmayr

[Genuinely high-dimensional nonlocality optimized by complementary measurements](#)

James Lim, Junghee Ryu, Seokwon Yoo et al.

[Open-system dynamics of entanglement: a key issues review](#)

Leandro Aolita, Fernando de Melo and Luiz Davidovich

[Characterizing entanglement with geometric entanglement witnesses](#)

Philipp Krammer

[Entanglement witnesses: construction, analysis and classification](#)

Dariusz Chruściński and Gniewomir Sarbicki

[Partial scaling transform of multiqubit states as a criterion of separability](#)

C Lupo, V I Man'ko, G Marmo et al.

[Entanglement of Lambda-atom and thermal photons in a double-band photonic crystal](#)

N Foroozani and M M Golshan

[Precise quantum tomography of photon pairs with entangled orbital angular momentum](#)

B Jack, J Leach, H Ritsch et al.

Complementarity reveals bound entanglement of two twisted photons

Beatrix C Hiesmayr^{1,2,4} and Wolfgang Löffler³

¹ Institute of Theoretical Physics and Astrophysics, Masaryk University, Kotlářská 2, 61137 Brno, Czech Republic

² University of Vienna, Faculty of Physics, Boltzmanngasse 5, A-1090 Vienna, Austria

³ Leiden University, Quantum Optics and Quantum Information, PO Box 9500, 2300-RA Leiden, Netherlands

E-mail: beatrix.hiesmayr@univie.ac.at

New Journal of Physics **15** (2013) 083036 (15pp)

Received 3 June 2013

Published 20 August 2013

Online at <http://www.njp.org/>

doi:10.1088/1367-2630/15/8/083036

Abstract. We demonstrate the detection of bipartite bound entanglement as predicted by the Horodecki's in 1998. Bound entangled states, being heavily mixed entangled quantum states, can be produced by incoherent addition of pure entangled states. Until 1998 it was thought that such mixing could always be reversed by entanglement distillation; however, this turned out to be impossible for bound entangled states. The purest form of bound entanglement is that of only two particles, which requires higher-dimensional ($d > 2$) quantum systems. We realize this using photon qutrit ($d = 3$) pairs produced by spontaneous parametric downconversion, that are entangled in the orbital angular momentum degrees of freedom, which is scalable to high dimensions. Entanglement of the photons is confirmed via a 'maximum complementarity protocol'. This conceptually simple protocol requires only maximized complementarity of measurement bases; we show that it can also detect bound entanglement. We explore the bipartite qutrit space and find that, also experimentally, a significant portion of the entangled states are actually bound entangled.

⁴ Author to whom any correspondence should be addressed.



Content from this work may be used under the terms of the [Creative Commons Attribution 3.0 licence](https://creativecommons.org/licenses/by/3.0/). Any further distribution of this work must maintain attribution to the author(s) and the title of the work, journal citation and DOI.

Contents

1. The maximum complementarity protocol	3
2. Three-dimensional orbital-angular-momentum entangled photons and bound entanglement	5
3. Maximum complementarity protocol	6
4. State tomography and magic simplex	7
5. Generality of the maximum complementarity protocol	9
6. Discussion	9
Acknowledgments	10
Appendix	10
References	13

The boundary between a classical and quantum world is the domain of mixed quantum states. Quantum entanglement of mixed states is much more complex than that of pure states and the subject of intense research. In 1998, it was found that entanglement of mixed states is not ‘flat’, but has an intriguing structure [1]: entangled quantum states can be classified into two distinct types, those that can and those that cannot be distilled into pure entangled states using stochastic local operations and classical communication. Undistillable entangled states are called bound entangled. Bound entanglement can occur in bipartite systems with dimensions larger than $d = 2$ or in the case of more particles. These two different types of bound entanglement differ considerably. The case of more than two entangled qubits has recently been realized experimentally in photonic multipartite systems [2–4], trapped ions [5] and NMR [6]; further, there is a study in a continuous-variable context [7] and a study of bound entanglement in thermal states for harmonic oscillator systems [8]. These results on multipartite qubit bound entanglement are interesting for certain quantum information tasks, e.g. reduction of the communication complexity [9] or secure key generation [10].

We investigate here the case of bound entanglement of *only two* photonic qutrits ($d = 3$) using the orbital angular momentum degree of freedom of light; this is the simplest case of bound entanglement and complications, such as those that occur for multipartite systems [11], do not occur. The orbital angular momentum of photons [12, 13] is used in a number of studies to obtain high-dimensional bipartite entangled qudits [14–17]. Apart from fundamental questions such as those discussed here, the system shows promise in quantum cryptography [18] due to improved security, increased resistance against noise and higher bit rates [19–22] compared to qubits.

In particular for such higher-dimensional qudit systems, it is well known that it is extremely hard to check whether a given state, especially if it is mixed—the daily situation in a laboratory—is separable or entangled. There are several operational criteria available to detect entanglement, where the most famous and powerful one is the Peres–Horodecki criterion, which is based on the partial transposition in one subsystem [23, 24]. After partial transposition, either all eigenvalues remain positive (PPT), or in the other case, if at least one eigenvalue is found to be negative, the state is entangled. The transposition of a state can be considered as synonymous to time reversal [25], so PPT tests if a state where time’s arrow is reversed for one of its partitions is still a physical state: obviously, if the state is separable, this must be the case. For two qubits, the reverse is also true and PPT is a sufficient criterion for separability.


"The Maximum Complementarity Protocol"			
			Correlation functions:
1. Step	Outcomes of Observable A_1 $\{0_1, 1_1, \dots, (d-1)_1\}$	Outcomes of Observable B_1 $\{0_1, 1_1, \dots, (d-1)_1\}$	$C_{A_1, B_1} = \sum_{i=0}^{d-1} \text{Tr}(i_1 i_1\rangle\langle i_1 i_1 \rho_d)$
2. Step	Outcomes of Observable A_2 $\{0_2, 1_2, \dots, (d-1)_2\}$	Outcomes of Observable B_2 $\{0_2, 1_2, \dots, (d-1)_2\}$	$C_{A_2, B_2} = \sum_{i=0}^{d-1} \text{Tr}(i_2 i_2\rangle\langle i_2 i_2 \rho_d)$
\vdots	\vdots	\vdots	\vdots
(d+1).Step	Outcomes of Observable A_{d+1} $\{0_{d+1}, 1_{d+1}, \dots, (d-1)_{d+1}\}$	Outcomes of Observable B_{d+1} $\{0_{d+1}, 1_{d+1}, \dots, (d-1)_{d+1}\}$	$C_{A_{d+1}, B_{d+1}} = \sum_{i=0}^{d-1} \text{Tr}(i_{d+1} i_{d+1}\rangle\langle i_{d+1} i_{d+1} \rho_d)$
			$I_{d+1} = \sum_{k=1}^{d+1} C_{A_k, B_k} \leq 2$

Figure 1. The steps involved in the complementarity protocol for entanglement detection of bipartite qudits. Alice and Bob determine the experimental probability (coincidence counts) for each detection state, and that for all (mutually unbiased) bases. It is then simply a matter of summing up these probabilities, if the sum is >2 , the state is entangled. Note that both Alice and Bob are allowed to relabel their measurement outcomes per basis, in order to optimize the detection ability.

This argument already fails for two qutrits, where it turns out that bound entangled qutrits are PPT. This brings us back to distillability: it was found that it is actually the positivity under partial transposition that makes bound entangled states undistillable [1]. Note that it is still open whether bound entangled states that are not PPT exist (see e.g. [26, 27]), since the PPT is only a sufficient but not necessary criterion for non-distillability.

We firstly explain our protocol that uses ‘maximum complementarity’ to detect entanglement (figure 1). Then we use experimentally photons that are entangled in their orbital angular momentum degrees of freedom to simulate a bound entangled bipartite state, on which we then apply the maximum complementarity protocol using sets of complementary observables to directly witness the inseparability. Finally, we verify the positivity under partial transposition via state tomography and, consequently, show that the detected state is indeed bound entangled.

1. The maximum complementarity protocol

Consider the following scenario of a source producing two-qudit states $\rho \in \mathbb{C}^{d \times d}$, namely quantum states with d degrees of freedom per qudit. Both experimenters, Alice and Bob, can choose among k different observables. What is the best strategy for Alice and Bob to detect the inseparability? The most striking difference between entanglement and separability are revealed by correlations in different basis choices. A fully correlated system is a physical system for which we can predict with certainty the outcome of a second measurement when we know the outcome of a first measurement, opposite to the other extreme case when knowledge of the first

measurement outcome does not reveal any information about the second measurement outcome. We would call this a fully uncorrelated system. Let us quantify this statement via a correlation function for two observables given in the spectral decomposition, A_k and B_k measured by Alice and Bob (with respective eigenvectors $\{|i_k\rangle\} = \{|0_k\rangle, \dots, |d-1_k\rangle\}$) by summing all *joint probabilities* $P_{A_k, B_k}(i_k, i_k)$ when both parties have the same outcome i_k

$$C_{A_k, B_k} = \sum_{i=0}^{d-1} P_{A_k, B_k}(i_k, i_k) = \sum_{i=0}^{d-1} \text{Tr}(|i_k i_k\rangle \langle i_k i_k| \rho_d). \quad (1)$$

Here, we allow Alice and Bob to relabel their outcomes such that C becomes maximal. Indeed the above function is a *mutual predictability*, since if the state is fully correlated then the outcomes can always be labelled such that $C = 1$, and if fully uncorrelated then any relabelling can only give $C = 1/d$ since all d outcomes are equally likely. However, this function does not tell us anything about entanglement, clearly the colour of the socks of Professor Bertlmann [28], who has the habit of wearing differently coloured socks, are also fully (anti-) correlated. Therefore, in a second step, Alice and Bob will now use the fundamental concept of complementarity and choose a second set of observables that are mutually unbiased to the first choices of observables A_1 and B_1 , namely the observables A_2 and B_2 . One way to phrase Bohr's complementarity of two observables A_1, A_2 is to say that they do not share any common eigenvector. This implies that the uncertainties of the outcomes are bounded by the scalar product of the eigenvectors of both observables and it is maximal if (and only if) all scalar products satisfy

$$|\langle i_n | j_m \rangle|^2 = \frac{1}{d} \quad \forall i, j \in \{0, 1, \dots, d-1\}. \quad (2)$$

This is also the defining property for two mutually unbiased bases (MUBs) [29] n and m , if $|i_n\rangle$ and $|i_m\rangle$ are their orthonormal basis vectors. Thus, predictabilities of a product state $|0_1 0_1\rangle$ are given by

$$\begin{aligned} P_{A_1, B_1}(i_1, i_1) &= \delta_{i,0}, \\ P_{A_2, B_2}(i_2, i_2) &= \text{Tr}(|i_2 i_2\rangle \langle i_2 i_2| 0_1 0_1\rangle \langle 0_1 0_1|) \\ &\stackrel{\text{equation (2)}}{=} \underbrace{|\langle 0_1 | i_2 \rangle|^2}_{\frac{1}{d}} \cdot \underbrace{|\langle 0_1 | i_2 \rangle|^2}_{\frac{1}{d}} = \frac{1}{d^2}, \end{aligned} \quad (3)$$

which holds for all i and we obtain for the correlation functions $C_{A_1, B_1} = 1$ and $C_{A_2, B_2} = \frac{1}{d}$. For a third choice of mutually complementary observables we obtain again $\frac{1}{d}$. In general, by adding up m correlation functions we obtain

$$I_m := \sum_{k=1}^m C_{A_k, B_k} \leq 1 + (m-1) \frac{1}{d} \quad (4)$$

that has to hold for all pure separable states. In [30] we have shown that it is also valid for all mixed separable states. Therefore, I_k serves as a detection function of entanglement if and only if the bound is not satisfied.

The existence of complete sets of MUBs in arbitrary dimensions is an open problem, but in the case of prime-power dimensions d it is known that there exist $d+1$ MUBs [29], thus

equation (4) becomes

$$I_{d+1}^{\text{equation (4)}} = \sum_{k=1}^{d+1} C_{A_k, B_k} \leq 2. \quad (5)$$

This detection criterion is not an entanglement measure but is very powerful, e.g. it detects all the entanglement of bipartite isotropic states, i.e. mixtures of a maximally entangled Bell state with the totally mixed state, as well as distinct types of multipartite entangled states [30]. Let us remark that our method of maximum complementarity provides a test for non-separability of a state whereas Bell inequalities can serve as an entanglement test but are designed to test for local realism. Indeed, so far only multipartite bound entangled states were found to violate a Bell inequality [31], while the question is still open for bipartite bound entangled states.

2. Three-dimensional orbital-angular-momentum entangled photons and bound entanglement

Now, we demonstrate both theoretically and experimentally that I_{d+1} is also capable of detecting bound entanglement for a certain class of so-called magic simplex states or Bell-diagonal states in 3×3 dimensions.

For the experimental test, we have chosen to use orbital-angular-momentum (OAM) [12] entangled photons generated by spontaneous parametric downconversion (SPDC). OAM entanglement [14, 15, 32, 33] is one implementation of spatial entanglement which is particularly intuitive because the quantum correlations of the photon pair are determined only by conservation of OAM during pair generation: the OAM quantum numbers ℓ_A and ℓ_B of the downconverted photons must fulfil $\ell_A + \ell_B = 0$ if the pump is a flat (Gaussian) beam with $\ell = 0$ [14, 34]. In the OAM basis $|\ell_A, \ell_B\rangle$ the two-photon qutrit state as produced by the crystal is

$$|\Psi_{\text{SPDC}}\rangle = \frac{1}{\sqrt{3}} \{ |-1, +1\rangle + |0, 0\rangle + |+1, -1\rangle \}. \quad (6)$$

In the following, we denote the states $\{|\ell = -1\rangle, |\ell = 0\rangle, |\ell = +1\rangle\}$ by $\{|0\rangle, |1\rangle, |2\rangle\}$. As a starting point we take the maximally entangled Bell state $P_{0,0} = |\Psi_{\text{SPDC}}\rangle\langle\Psi_{\text{SPDC}}|$ and, via applying the unitary Weyl operators $W_{k,l} := \sum_{n=0}^{d-1} e^{\frac{(2\pi i)(kn)}{d}} |n\rangle\langle n+l|$ in one subsystem (e.g. on the photon of Alice), we can synthesize the $d^2 - 1$ maximally entangled Bell states $P_{k,l} = W_{k,l} \otimes \mathbb{1} P_{0,0} W_{k,l}^\dagger \otimes \mathbb{1}$. Any convex combination of these d^2 Bell states forms a so called ‘magic simplex’ [35] $\mathcal{W} := \{\rho_d = \sum_{k,l=0}^{d-1} c_{k,l} P_{k,l} | c_{k,l} \geq 0, \sum_{l,k=0}^{d-1} c_{k,l} = 1\}$. This reduced state space of locally maximally mixed states admits a simple geometrical representation (the vertices are the d^2 Bell states) and has been shown [35–41] to be powerful in addressing inseparability issues and quantum information theoretic questions.

For our purpose let us reduce the $d^2 - 1$ dimensional parameter space to three (four in the case of $d > 3$) parameters q_i and consider the following family of states:

$$\begin{aligned} \rho_d = & \left(1 - \frac{q_1}{d^2 - (d+1)} - \frac{q_2}{d+1} - q_3 - (d-3)q \right) \frac{1}{d^2} \mathbb{1}_{d^2} + \frac{q_1}{d^2 - (d+1)} P_{0,0} + \frac{q_2}{(d+1)(d-1)} \\ & \times \sum_{i=1}^{d-1} P_{i,0} + \frac{q_3}{d} \sum_{i=0}^{d-1} P_{i,1} + (1 - \delta_{d,3}) \frac{q_4}{d} \sum_{z=2}^{d-2} \sum_{i=0}^{d-1} P_{i,z}. \end{aligned} \quad (7)$$

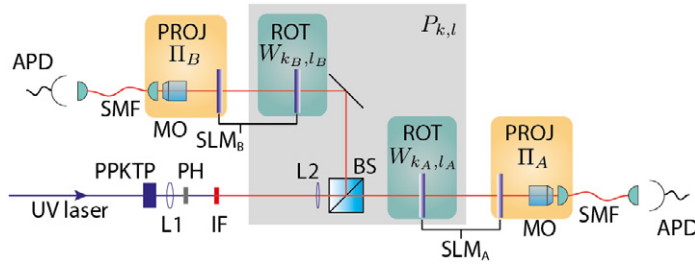


Figure 2. Experimental setup for measurement of bound-entangled bipartite qutrits. Photon pairs are created by downconversion (type-I) of 413 nm UV photons in a PPKTP crystal, momentum-filtered by a pinhole (PH) and split probabilistically using a beamsplitter (BS). ROT in the orbital angular momentum superposition mode-space for production of the Bell states $P_{k,l}$ (grey box) via $W_{k_{A/B},l_{A/B}}$ is performed using a SLM. Projective measurements (PROJ) are done by appropriate mode transformation and subsequent imaging onto the core of a single mode fibre (SMF) as indicated by $\Pi_{A/B}$. We have implemented both operations on the same SLM. The photons are guided to an avalanche photo diode (APD), and detection events belonging to an entangled photon pair are post-selected by coincidence detection.

This family also includes for $d = 3$ the one-parameter Horodecki-state, the first found bound entangled state [1]. Namely, for $q_1 = \frac{30-5\lambda}{21}$, $q_2 = -\frac{8\lambda}{21}$, $q_3 = \frac{5-2\lambda}{7}$ with $\lambda \in [0, 5]$. This state is PPT for $\lambda \in [1, 4]$ and was shown to be bound entangled for $\lambda \in (3, 4]$.

By expressing the totally mixed state $\mathbb{1}_9$ as the sum of all Bell states $\sum P_{k,l}$ we find that all nine Bell states need to be mixed to synthesize the state ρ_3 . Note that there are 72 unitary equivalent possibilities [35] to generate ρ_3 that we will exploit to deduce the error (see the appendix). We introduce a measurement-based scheme to produce these mixed states similar to the authors in [2–4, 42, 43] for polarization, but in our case for OAM qutrits using spatial light modulation, see figure 2 to apply single-qutrit rotations (ROTs) (e.g. on qutrit A) using the Weyl matrix $W_{k,l}$ to transform $P_{0,0}$ into any of the eight other maximally entangled Bell states $P_{k,l}$. This operation is implemented on the spatial light modulators (SLMs, see figure 2), which allows us to generate the mixed state by time-multiplexing of the ROT operators $W_{k,l}$ for a particular choice of q_i . Our method is physically equivalent to tracing over a separate degree of freedom to create decoherence, such as the spectral one, a method which has also been used to generate mixed states [44, 45] or stochastic ROT with an additional optical element [2–4, 42, 43]. In our case we extend this to obtain full control over the high-dimensional mixture by using retroactive mixing: we record photon counts for each of the states $P_{k,l}$, and form the incoherent summation. If Bob and Alice are given this experimental data, they cannot reverse the procedure since a test does not exist to distinguish in which way the mixing was done nor in which way the mixed state was created at all.

3. Maximum complementarity protocol

In a first step we want to verify entanglement of the state, shown in figure 4, directly by using the complementarity protocol. For that, the correlation functions have to be

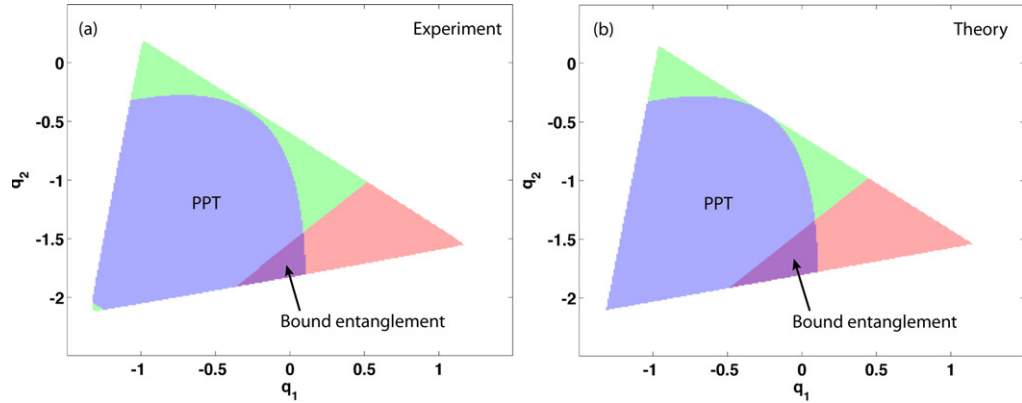


Figure 3. Experimental (a) and theoretical (b) 2D slice $\{q_1, q_2\}$ through the magic simplex for fixed $q_3 = -0.5776$. All coloured points correspond to states having positive semidefinite eigenvalues, therefore representing physical states. The blue area (curved region) covers the range of states with a positive partial transpose (PPT). The red triangular area indicates where the maximum complementarity protocol applied to the experimentally generated states (a) or theoretical states (b) is greater than 2, thus detecting entanglement. States where all three conditions are fulfilled are bound entangled. We see that the experimental and theoretical geometries agree very well.

measured directly, which is considered to be difficult due to normalization: we have to obtain probabilities directly from experimental coincidence rates. We obtain the probabilities P from the normalized coincidence rates Γ via $P_{A_k, B_k}(i_k, i_k) = \Gamma_{A_k, B_k}(i_k, i_k) / \sum_{s_k, t_k} \Gamma_{A_k, B_k}(s_k, t_k)$. From this we calculate the correlation functions C given the state described in figure 4 and obtain:

Correlation function	Theory	Experiment
C_{A_1, B_1}	0.675	0.667 ± 0.005
C_{A_2, B_2}	0.468	0.463 ± 0.005
C_{A_3, B_3}	0.468	0.469 ± 0.005
C_{A_4, B_4}	0.468	0.467 ± 0.005
$2 - (I_4 = \sum_k C_{A_k, B_k})$	-0.079	-0.066 ± 0.02

The experimental uncertainties (standard deviations) are determined from multiple experimental runs. Experiment and theory agree well, therefore the maximum complementary protocol confirms that we detect a truly entangled state.

4. State tomography and magic simplex

We perform quantum state tomography [46] of the entangled state and then show that it is bound entangled by applying the Peres–Horodecki criterion. We keep $q_3 = -0.5776$ fixed, this allows us to visualize quantum state properties in 2D: figure 3 shows the experimental

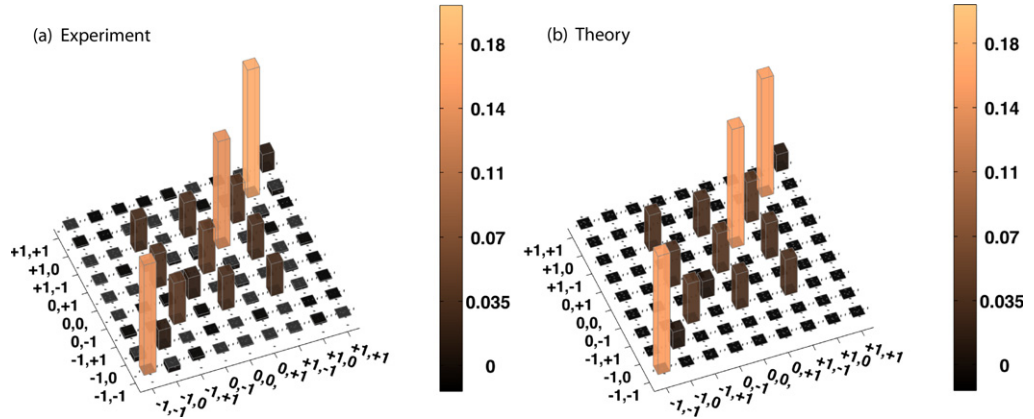


Figure 4. Experimental (a) and theoretical (b) real parts of the density matrices of the bound entangled state ($q_1 = -0.07$, $q_2 = -1.73$, $q_3 = -0.5774$). The fidelity of the experimental state is 0.98, the complementarity protocol applied to the experimental state gives $2 - I_{d+1} = -0.032 \pm 0.003$ and the minimum eigenvalue of the partially transposed state is $\text{Min}[\text{eig}(\rho^{T_A})] = +0.0101 \pm 0.0017$; the state is bound entangled. It is expected to be purely real; the experimental imaginary parts are all below 10%. The axes labels indicate the OAM quantum numbers ℓ .

(a) and theoretical case (b), where each coloured pixel $\{q_1, q_2\}$ corresponds to a state, blue if PPT (curved region) and red if the state violates the maximum complementarity protocol, $2 - I_{d+1} < 0$ (triangle). In regions where all conditions are fulfilled, we have non-separable states with a positive partial transposition, i.e. bound entanglement. We find that, compared to the total area of physical states, the bound entangled states occupy a significant space in the chosen slice through the magic simplex; the extension along q_3 turns out to be even much larger, i.e. the bound entangled states occupies a rather large volume. Since the regions in figure 3 are simply connected ('they do not have holes'), it is obvious from the geometry that states within the region where all criteria apply are bound entangled. However, it is important to check that the conditions are also fulfilled significantly [11]. In contrast to the polarization qubit case [2], in spatial entanglement, the most important errors are due to wavefront aberrations that lead to a small ROT of the state in the Hilbert space. Because we have access to all 72 unitary-equivalent states of ρ_3 (see the appendix), we can calculate for each of them the complementarity protocol $2 - I_{d+1}$ and the smallest eigenvalue of the partially transposed state $\text{Min}[\text{eig}(\rho^{T_A})]$ to derive the mean values and standard deviations. In figure 4 we plot explicitly the matrix elements of the bound entangled state ($q_1 = -0.07$, $q_2 = -1.73$, $q_3 = -0.5774$) together with the theoretical prediction. The numerical values are $2 - I_{d+1} = -0.032 \pm 0.003$ and $\text{Min}[\text{eig}(\rho^{T_A})] = +0.0101 \pm 0.0017$. This clearly proves that the state is bound entangled: non-separable, but PPT.

We also studied the historical Horodecki-state [1], and we can indeed confirm bound entanglement thereof for a large range of the λ -parameter. For instance, for $\lambda = 3.5$, we get $2 - I_{d+1} = -0.025 \pm 0.003$, and $\text{Min}[\text{eig}(\rho^{T_A})] = +0.012 \pm 0.002$.

5. Generality of the maximum complementarity protocol

Let us discuss what we would expect for the case of higher dimensional OAM entangled photons in the state ρ_d . We search the parameter space of prime and prime-power dimensional entangled states (the dimensions where $d + 1$ MUBs are known), and optimize our maximum complementarity protocol to find the states where the detection of entanglement via $2 - I_{d+1}$ is strongest:

$$\min_{q_i, \rho_d \geq 0, \rho_d^{T_A} \geq 0} 2 - I_{d+1}[\rho_d] = \begin{cases} -0.15 \ (d = 3), \\ -0.125 \ (d = 4), \\ -0.106 \ (d = 5), \\ -0.081 \ (d = 7), \\ -0.073 \ (d = 8), \\ -0.067 \ (d = 9). \end{cases} \quad (8)$$

In each case, a similar geometry as shown in figure 3 is obtained (for details, see [35, 36]). In dimension $d = 2 \times 3 = 6$ so far only three MUBs are found and there are strong numerical hints [29] that nothing more exists; applying only these three MUBs does not lead to the detection of bound entanglement.

We turn now to the multipartite case. In [47] we have shown via geometry considerations that if a Hermitian operator detects entanglement of states in a certain quantum space \mathcal{W} , then it also detects entanglement in the multi-partite product space $\mathcal{W}^{\otimes n} := \{\rho_{d,\otimes n} = \sum c_{k,l} \tilde{P}_{k,l} | c_{k,l} \geq 0, \sum c_{k,l} = 1\}$. Also in this case, the d^2 Bell-type vertex states $\tilde{P}_{k,l}$ are obtained by applying a Weyl operator in one subsystem to $\tilde{P}_{0,0} = \frac{1}{d^2} \sum P_{k,l}^{\otimes n}$. Therefore, the maximum complementarity protocol is also applicable for multipartite states and can detect bound entanglement as well as PPT entanglement therein (see below).

To illustrate the richness and difference between bipartite and multipartite bound entanglement, let us discuss first the famous case of $d = 2$. Then the vertex states are the Smolin states [48] that are known to be multiparticle ununlockable bound entangled, because no local party can distil entanglement; however, *two* parties can distil (unlock) the entanglement, which would in this case actually be a pure maximally entangled state; but it is only available for the other parties not themselves. This case was recently experimentally demonstrated [2, 3]. Surprisingly, entangled states inside the magic simplex $\mathcal{W}^{\otimes n}$ can be distilled to the Smolin-type vertex states [47], which themselves are undistillable. For $d > 2$, in addition, the multipartite magic simplex contains PPT-entangled states, therefore, states that cannot even be purified to a vertex state. They are bound entangled and only unlockable due to their multiparticle nature. We emphasize that bipartite bound entangled states, such as those investigated here, are fundamentally distinct from multipartite bound entangled states because entanglement unlocking to obtain pure bipartite entanglement generation is impossible if only two parties are present.

6. Discussion

We observed the 1998-predicted bipartite bound entanglement in the orbital angular momentum degrees of freedom of two photons. Entanglement was confirmed with the maximum

complementarity protocol that is only based on the existence of complementary observables. This itself is surprising since most methods, such as PPT, fail to detect bound entanglement, and it raises the question why maximal correlations in different basis choices can reveal irreversible bound entanglement in the first place.

We have chosen orbital angular momentum entanglement of photons that is scalable in the dimensionality [15], and our high-quality results suggest that further exploration of high dimensional entangled quantum states is possible. Therefore, our experimental method and the maximum complementarity protocol is a useful addition to the toolbox to explore different types of entanglement including bound entanglement. With the case of two qutrits as the most simple system we lay the foundation to also pursue experimentally the question of why Nature should provide us with such a strange form of highly mixed entanglement that can not be purified: what is its physical meaning?

Finally, via application of the maximum complementarity protocol we confirmed experimentally that the maximum number of MUBs in a complete set cannot be more than $d + 1$: If for families of states that are optimally detected by I_{d+1} , another MUB would be added (i.e. $m > d + 1$ in equation (4)), we would have detected separable states as entangled ones [30], which is not the case. The minimum number of existing MUBs is known to be the smallest of the prime factors of d plus one. It is also open whether one always needs all MUBs to detect bound entanglement. Consequently, investigating inseparability problems opens a different trail to look for a solution of the number problem of MUBs, i.e. how many MUBs are needed for a complete set.

Acknowledgments

We thank R A Bertlmann and A Gabriel for discussions and acknowledge the SoMoPro programme, NWO, Austrian Science Fund (FWF-P23627-N16), and the EU STREP programme 255914 (PHORBITECH). The project is funded from the SoMoPro programme. Research of BCH leading to these results has received financial contribution from the European Community within the Seventh Framework Programme (FP/2007-2013) under grant agreement no. 229603. The research is also co-financed by the South Moravian Region. WL acknowledges support from NWO and the EU STREP program 255914 (PHORBITECH).

Appendix

A.1. Maximum complementarity protocol

As an explicit example we show our choice of basis vectors of the four MUBs \mathcal{B}_k with $w = e^{\frac{2\pi i}{3}}$:

$$\mathcal{B}_1 : \{|0_1\rangle, |1_1\rangle, |2_1\rangle\} = \left\{ \begin{pmatrix} 1 \\ 0 \\ 0 \end{pmatrix}, \begin{pmatrix} 0 \\ 1 \\ 0 \end{pmatrix}, \begin{pmatrix} 0 \\ 0 \\ 1 \end{pmatrix} \right\},$$

$$\mathcal{B}_2 : \{|0_2\rangle, |1_2\rangle, |2_2\rangle\} = \frac{1}{\sqrt{3}} \left\{ \begin{pmatrix} 1 \\ 1 \\ 1 \end{pmatrix}, \begin{pmatrix} 1 \\ w \\ w^2 \end{pmatrix}, \begin{pmatrix} 1 \\ w^2 \\ w \end{pmatrix} \right\},$$

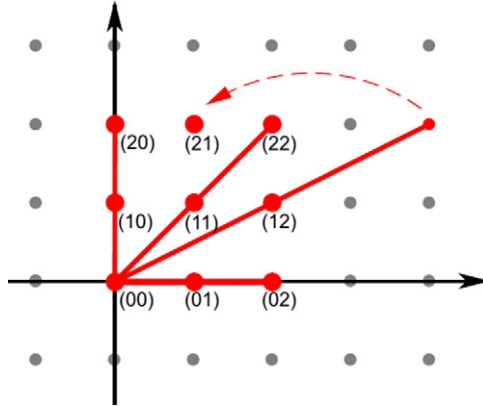


Figure A.1. Illustration of the finite discrete classical phase space for dimension $d = 3$ of the locally maximally mixed states of the magic simplex \mathcal{W} . Each point (kl) represent one of the nine Bell states $P_{k,l}$. All possible complete lines through the point (00) for $d = 3$ are drawn, representing one class of states which have the same geometry concerning separability, bound entanglement, free entanglement and nonlocality, i.e. those that are unitary equivalent. The same holds for each line which is parallel to any red line.

$$\mathcal{B}_3 : \{|0_3\rangle, |1_3\rangle, |2_3\rangle\} = \frac{1}{\sqrt{3}} \left\{ \begin{pmatrix} 1 \\ w \\ w \end{pmatrix}, \begin{pmatrix} 1 \\ w^2 \\ 1 \end{pmatrix}, \begin{pmatrix} 1 \\ 1 \\ w^2 \end{pmatrix} \right\},$$

$$\mathcal{B}_4 : \{|0_4\rangle, |1_4\rangle, |2_4\rangle\} = \frac{1}{\sqrt{3}} \left\{ \begin{pmatrix} 1 \\ w^2 \\ w^2 \end{pmatrix}, \begin{pmatrix} 1 \\ 1 \\ w \end{pmatrix}, \begin{pmatrix} 1 \\ w \\ 1 \end{pmatrix} \right\}.$$

To detect (bound) entanglement, we choose the following combination of correlation functions ($|i^*\rangle = |i\rangle^*$):

$$C_{A_1, B_1} = \sum_{i=0}^2 \text{Tr}(|i_1, \text{mod}(i_1 + 2, 3)^*\rangle \langle i_1, \text{mod}(i_1 + 2, 3)^*| \rho_3),$$

$$C_{A_k, B_k} = \sum_{i=0}^2 \text{Tr}(|i_k, i_k^*\rangle \langle i_k, i_k^*| \rho_3), \quad k = 2, 3, 4.$$

A.2. Phase space of two qutrits

Below, in figure A.1, the finite phase space of the magic simplex [35] is drawn for dimension $d = 3$. This space is spanned by all nine Bell states $P_{k,l}$, which can be generated by applying the Weyl operators $W_{k,l}$ onto one arbitrary maximally entangled Bell state, denoted by $P_{0,0}$: $P_{k,l} = W_{k,l} \otimes \mathbb{1} P_{0,0} W_{k,l}^\dagger \otimes \mathbb{1}$. Due to the group structure of the Weyl operators certain mixtures of the Bell states $P_{k,l}$ are geometrically equivalent, i.e. have the same properties concerning

separability, bound entanglement, free entanglement and nonlocality (violation of a given Bell inequality). Thus one has not to analyse all possible mixtures since some are equivalent concerning the properties we are interested in. In particular, the so called *lines* are special. A line is formed by choosing one Bell state, e.g. $P_{0,0}$, and applying to it $d-1$ times the same Weyl operator, e.g. $W_{0,1}$. Applying another time, the Weyl operator brings one back to the original state (in our case $P_{0,0}$), because of the periodicity of the Weyl operators. In our case the three Bell states $\{P_{0,0}, P_{0,1}, P_{0,2}\}$ form a line in the phase space (see figure A.1). We find $d+1$ lines with different orientations through one Bell state $P_{0,0}$ (red lines in figure A.1). To each (red) line there are three parallel lines. In summary, we find $(3+1) \times 3 = 12$ lines, which have the same geometry regarding separability, bound entanglement, free entanglement, and nonlocality.

For our state ρ_3 (equation (7)), we see that the states weighted by q_1 and q_2 form a line and q_3 is the coefficient for another line that is parallel to the first one. Thus, we have $(3+1) \times 3$ possibilities to choose a line and three possibilities to weight them with q_1 and q_2 . And there are two possibilities to choose parallel lines to the chosen one weighted by q_3 . Thus we have in total $(3+1) \times 3 \times 3 \times 2 = 72$ unitary equivalent possibilities to obtain the state ρ_3 , and all of these have in theory the same geometry regarding separability, bound entanglement, free entanglement and nonlocality.

A.3. Experiment

We generate the spatially entangled photon pairs by collinear Type-I SPDC of a fundamental Gaussian laser beam in a 2 mm long nonlinear PPKTP (periodically poled potassium titanyl phosphate) crystal (Krypton-ion pump laser at $\lambda = 413$ nm wavelength, Gaussian beam waist at crystal $w_p = 325 \mu\text{m}$, 80 mW power). The phase-matching in the crystal is tuned via temperature control to produce a similar amount of downconverted photons in the $\ell = 0$ and ± 1 OAM mode. We image the crystal surface with $7.5\times$ magnification using a telescope onto the SLM (Hamamatsu X10468-07) surface, see figure 2. The SLM is operated under an incident angle of 10° or 5° ; this allows us to use a single SLM for both signal and idler photon. The (phase-corrected) SLM is used with a first-order blaze angle of 1 mrad, and other orders are eliminated with a PH. The far field of the SLM surface is sent to the SMF using $10\times$ objectives, with a detection-fibre mode waist at the SLM of $1275 \mu\text{m}$. The fibres are connected to single-photon counters and we post-select photon pairs by coincidence detection (7 ns time window). All measurements were integrated for 2 s; we obtain typically 30 000 single counts and 1500 coincidence counts for conjugated-field detector settings and <10 coincidence counts for the cases where no coincidence events are expected. The combination of field modulation via the SLM and SMF projection allows for PROJs in the OAM basis. The SLM kinoforms required for two-state superpositions involve only phase modulation, however, for three-state superpositions such as those used for implementation of the maximum complementarity protocol, require additional spatial amplitude modulation. Because this is very inefficient if done in a continuous way [15], we employ binary amplitude modulation by removing the blaze at spatial positions where the normalized modulus of the detection field amplitude is smaller than $\sqrt{0.5}$. For tomographic reconstruction, we obtain an overcomplete set of measurements by detecting all two-state superpositions with relative phases of $\{0, \pi/2, \pi, 3\pi/2\}$.

A.4. Experimental error estimation

In the experiment, the nine Bell states that constitute the bound entangled state are not fully unitary equivalent due to errors, mainly due to small wavefront aberrations. These aberrations lead to ROTs in the two-photon Hilbert space. A consequence of this is that all 72 unitary-equivalent versions of ρ_3 (see above section A.2) are slightly different and lead to slightly different values for the complementarity protocol ($2 - I_{d+1}$) and the minimum eigenvalue of the partial transpose ($\text{Min}[\text{eig}(\rho^{TA})]$). For realistic estimation of the experimental accuracy, we determine the quantities for all 72 unitary-equivalent states and calculate the standard deviation. Statistical errors due to photon shot noise are not relevant here because we average over sufficient many detection events.

References

- [1] Horodecki M, Horodecki P and Horodecki R 1998 Mixed-state entanglement and distillation: is there a ‘bound’ entanglement in nature? *Phys. Rev. Lett.* **80** 5239–42
- [2] Amselem E and Bourennane M 2009 Experimental four-qubit bound entanglement *Nature Phys.* **5** 748–52
- [3] Lavoie J, Kaltenbaek R, Piani M and Resch K J 2010 Experimental bound entanglement in a four-photon state *Phys. Rev. Lett.* **105** 130501
- [4] Kaneda F, Shimizu R, Ishizaka S, Mitsumori Y, Kosaka H and Edamatsu K 2012 Experimental activation of bound entanglement *Phys. Rev. Lett.* **109** 040501
- [5] Barreiro J T, Schindler P, Gühne O, Monz T, Chwalla M, Roos C F, Hennrich M and Blatt R 2010 Experimental multiparticle entanglement dynamics induced by decoherence *Nature Phys.* **6** 943–6
- [6] Kampermann H, Bruß D, Peng X and Suter D 2010 Experimental generation of pseudo-bound-entanglement *Phys. Rev. A* **81** 040304
- [7] DiGuglielmo J, Samblowski A, Hage B, Pineda C, Eisert J and Schnabel R 2011 Experimental unconditional preparation and detection of a continuous bound entangled state of light *Phys. Rev. Lett.* **107** 240503
- [8] Ferraro A, Cavalcanti D, García-Saenz A and Acín A 2008 Thermal bound entanglement in macroscopic systems and area law *Phys. Rev. Lett.* **100** 080502
- [9] Epping M and Brukner Č 2013 Bound entanglement helps to reduce communication complexity *Phys. Rev. A* **87** 032305
- [10] Augusiak R and Horodecki P 2009 W-like bound entangled states and secure key distillation *Europhys. Lett.* **85** 50001
- [11] Lavoie J, Kaltenbaek R, Piani M and Resch K J 2010 Experimental bound entanglement? *Nature Phys.* **6** 827–7
- [12] Allen L, Beijersbergen M W, Spreeuw R J C and Woerdman J P 1992 Orbital angular momentum of light and the transformation of Laguerre–Gaussian laser modes *Phys. Rev. A* **45** 8185–9
- [13] Molina-Terriza G, Torres J P and Torner L 2007 Twisted photons *Nature Phys.* **3** 305–10
- [14] Mair A, Vaziri A, Weihs G and Zeilinger A 2001 Entanglement of the orbital angular momentum states of photons *Nature* **412** 313–6
- [15] Dada A C, Leach J, Buller G S, Padgett M J and Andersson E 2011 Experimental high-dimensional two-photon entanglement and violations of generalized Bell inequalities *Nature Phys.* **7** 677–80
- [16] Salakhutdinov V D, Eliel E R and Löffler W 2012 Full-field quantum correlations of spatially entangled photons *Phys. Rev. Lett.* **108** 173604
- [17] Shalm L K, Hamel D R, Yan Z, Simon C, Resch K J and Jennewein T 2013 Three-photon energy-time entanglement *Nature Phys.* **9** 19–22

- [18] Bechmann-Pasquinucci H and Peres A 2000 Quantum cryptography with 3-state systems *Phys. Rev. Lett.* **85** 3313–6
- [19] Kaszlikowski D, Gnaniński P, Zukowski M, Miklaszewski W and Zeilinger A 2000 Violations of local realism by two entangled n -dimensional systems are stronger than for two qubits *Phys. Rev. Lett.* **85** 4418–21
- [20] Fujiwara M, Takeoka M, Mizuno J and Sasaki M 2003 Exceeding the classical capacity limit in a quantum optical channel *Phys. Rev. Lett.* **90** 167906
- [21] Bechmann-Pasquinucci H and Tittel W 2000 Quantum cryptography using larger alphabets *Phys. Rev. A* **61** 062308
- [22] Durt T, Cerf N J, Gisin N and Zukowski M 2003 Security of quantum key distribution with entangled qutrits *Phys. Rev. A* **67** 012311
- [23] Peres A 1996 Separability criterion for density matrices *Phys. Rev. Lett.* **77** 1413–5
- [24] Horodecki M, Horodecki P and Horodecki R 1996 Separability of mixed states: necessary and sufficient conditions *Phys. Lett. A* **223** 1–8
- [25] Busch P and Lahti P J 1997 Remarks on separability of compound quantum systems and time reversal *Found. Phys. Lett.* **10** 113–7
- [26] Hofmann H F 2003 Bound entangled states violate a nonsymmetric local uncertainty relation *Phys. Rev. A* **68** 034307
- [27] Pankowski Ł, Piani M, Horodecki M and Horodecki P 2010 A few steps more towards npt bound entanglement *IEEE Trans. Inform. Theory* **56** 4085–100
- [28] Bell J 1981 Bertlmann's socks and the nature of reality *J. Physique Coll.* **42** C2-41–62
- [29] Durt T, Englert B, Bengtsson I and Życzkowski K 2010 On mutually unbiased bases *Int. J. Quantum Inform.* **8** 535–640
- [30] Spengler C, Huber M, Brierley S, Adaktylos T and Hiesmayr B C 2012 Entanglement detection via mutually unbiased bases *Phys. Rev. A* **86** 022311
- [31] Dür W 2001 Multipartite bound entangled states that violate Bell's inequality *Phys. Rev. Lett.* **87** 230402
- [32] Monken C H, Ribeiro P H S and Pádua S 1998 Transfer of angular spectrum and image formation in spontaneous parametric down-conversion *Phys. Rev. A* **57** 3123–6
- [33] Franke-Arnold S, Barnett S M, Padgett M J and Allen L 2002 Two-photon entanglement of orbital angular momentum states *Phys. Rev. A* **65** 033823
- [34] Walborn S P, de Oliveira A N, Thebaldi R S and Monken C H 2004 Entanglement and conservation of orbital angular momentum in spontaneous parametric down-conversion *Phys. Rev. A* **69** 023811
- [35] Baumgartner B, Hiesmayr B C and Narnhofer H 2006 State space for two qutrits has a phase space structure in its core *Phys. Rev. A* **74** 032327
- [36] Baumgartner B, Hiesmayr B and Narnhofer H 2007 A special simplex in the state space for entangled qudits *J. Phys. A: Math. Gen.* **40** 7919
- [37] Baumgartner B, Hiesmayr B and Narnhofer H 2008 The geometry of bipartite qutrits including bound entanglement *Phys. Lett. A* **372** 2190–5
- [38] Bertlmann R A and Krammer P 2009 Entanglement witnesses and geometry of entanglement of two-qutrit states *Ann. Phys.* **324** 1388–407
- [39] Chruściński D, Kossakowski A, Młodawski K and Matsuoka T 2010 A class of bell diagonal states and entanglement witnesses *Open Syst. Inform. Dyn.* **17** 213–31
- [40] Chruściński D and Kossakowski A 2010 Bell diagonal states with maximal abelian symmetry *Phys. Rev. A* **82** 064301
- [41] Chruściński D and Rutkowski A 2011 A family of generalized Horodecki-like entangled states *Phys. Lett. A* **375** 2793–6
- [42] Acin A 2009 Entanglement: entangled and bound *Nature Phys.* **5** 711–2
- [43] Dobek K, Karpiński M, Demkowicz-Dobrzański R, Banaszek K and Horodecki P 2011 Experimental extraction of secure correlations from a noisy private state *Phys. Rev. Lett.* **106** 030501

- [44] Peters N A, Altepeter J B, Branning D, Jeffrey E R, Wei T C and Kwiat P G 2004 Maximally entangled mixed states: creation and concentration *Phys. Rev. Lett.* **92** 133601
- [45] Puentes G, Voigt D, Aiello A and Woerdman J P 2006 Tunable spatial decoherers for polarization-entangled photons *Opt. Lett.* **31** 2057–9
- [46] James D F V, Kwiat P G, Munro W J and White A G 2001 Measurement of qubits *Phys. Rev. A* **64** 052312
- [47] Hiesmayr B C and Huber M 2009 Two distinct classes of bound entanglement: PPT-bound and ‘multi-particle’-bound arXiv:0906.0238
- [48] Smolin J A 2001 Four-party unlockable bound entangled state *Phys. Rev. A* **63** 032306